EDGEWOOD CHEMICAL BIOLOGICAL CENTER
U.S. ARMY RESEARCH, DEVELOPMENT AND ENGINEERING COMMAND
Aberdeen Proving Ground, MD 21010-5424

ECBC-TR-955

VAPOR-PHASE INFRARED SPECTRAL STUDY OF WEAPONS-GRADE O-ETHYL S-2-(DIISOPROPYLAMINO)ETHYL METHYLPHOSPHONOTHIOLATE (VX)

Barry R. Williams
Melissa S. Hulet

SCIENCE APPLICATIONS INTERNATIONAL CORPORATION
Gunpowder, MD 21010-0068

Alan C. Samuels
Ronald W. Miles, Jr.

RESEARCH AND TECHNOLOGY DIRECTORATE

May 2012

Approved for public release; distribution is unlimited.

U.S. ARMY RDECOM

Disclaimer

The findings in this report are not to be construed as an official Department of the Army position unless so designated by other authorizing documents.

REPORT DOCUMENTATION PAGE

Form Approved
OMB No. 0704-0188

Public reporting burden for this collection of information is estimated to everege 1 hour per response, including the time for reviewing instructions, searching existing deta sources, gathering and maintaining the data needed, and completing and raviewing this collection of information. Send comments regarding this burden estimate or any other aspect of this collection of information, including suggestions for reducing this burden to Department of Defense, Weshington Headquarters Services, Directorate for Information Operations and Reports (0704-0188), 1215 Jefferson Davis Highway, Suite 1204, Arlington, VA 22202-4302. Respondants should be aware that notwithstanding any other provision of law, no person shall be subject to any penalty for failing to comply with a collection of information if it does not display a currently valid OMB control number. **PLEASE DO NOT RETURN YOUR FORM TO THE ABOVE ADDRESS.**

1. REPORT DATE *(DD-MM-YYYY)*	2. REPORT TYPE	3. DATES COVERED *(From - To)*
XX-05-12	Final	Feb 2009 - Mar 2009

4. TITLE AND SUBTITLE
Vapor-Phase Infrared Spectral Study of Weapons-Grade O-Ethyl S-2-(diisopropylamino)ethyl methylphosphonothiolate (VX)

5a. CONTRACT NUMBER

5b. GRANT NUMBER

5c. PROGRAM ELEMENT NUMBER

6. AUTHOR(S)
Williams, Barry R.; Hulet, Melissa S. (SAIC); Samuels, Alan C.; and Miles, Ronald W., Jr. (ECBC)

5d. PROJECT NUMBER

5e. TASK NUMBER

5f. WORK UNIT NUMBER

7. PERFORMING ORGANIZATION NAME(S) AND ADDRESS(ES)
Science Applications International Corporation (SAIC), P.O. Box 68, Gunpowder, MD 21010-0068
DIRECTOR, ECBC, ATTN: RDCB-DRD-P, APG, MD 21010-5424

8. PERFORMING ORGANIZATION REPORT NUMBER
ECBC-TR-955

9. SPONSORING / MONITORING AGENCY NAME(S) AND ADDRESS(ES)

10. SPONSOR/MONITOR'S ACRONYM(S)

11. SPONSOR/MONITOR'S REPORT NUMBER(S)

12. DISTRIBUTION / AVAILABILITY STATEMENT
Approved for public release; distribution is unlimited.

13. SUPPLEMENTARY NOTES

14. ABSTRACT
We report the infrared spectra of weapons-grade O-ethyl-S-2-(diisopropylamino)ethyl methylphosphonothiolate in the mid-infrared (4000–550 cm^{-1}) region. The chemical used in the feedstock was obtained from a ton container and was analyzed by gas chromatography-mass spectrometry and nuclear magnetic resonance spectroscopy to determine its composition. Analysis of the data showed that the spectra were dominated by the volatile impurities in the VX, which were primarily acetone, 1,3-diisopropylcarbodiimide, and diisopropylamine. Concentrations of the compounds observed in the vapor were similar to the predictions made using Raoult's law. The availability of the absorptivity coefficients of most of the compounds found in the effluent enabled us to calculate a mass balance.

15. SUBJECT TERMS

Absorptivity coefficient	Vapor phase	FTIR
Saturator cell	Vapor pressure	VX
Quantitative	Byproduct	Degradant
O-Ethyl-S-2-(diisopropylamino)ethyl methylphosphonothiolate		Infrared

16. SECURITY CLASSIFICATION OF:			17. LIMITATION OF ABSTRACT	18. NUMBER OF PAGES	19a. NAME OF RESPONSIBLE PERSON
a. REPORT	b. ABSTRACT	c. THIS PAGE			Renu B. Rastogi
U	U	U	UL	48	19b. TELEPHONE NUMBER *(include area code)* (410) 436-7545

Standard Form 298 (Rev. 8-98)
Prescribed by ANSI Std. Z39.18

20120607072

Blank

EXECUTIVE SUMMARY

Current standoff detection protocols for the nerve agent, O-ethyl-S-2-(diisopropylamino)ethyl methylphosphonothiolate (VX), assume that the material is of high purity and that the spectra are dominated by VX in the vapor state. We report the acquisition of spectra of weapons-grade VX in the mid-infrared region at 23 °C. The chemical used to generate the spectra was obtained from a ton container that was analyzed by gas chromatography–mass spectrometry and nuclear magnetic resonance spectroscopy to determine its composition. In contrast to the pure component vapor-phase reference spectrum, obtained at 69 °C, analysis of the data from the weapons-grade material showed that the spectra were dominated by the volatile impurities in the VX—primarily acetone, 1,3-diisopropylcarbodiimide, and diisopropylamine. Concentrations of the compounds observed in the vapor were similar to the predictions made using Raoult's law. The availability of the absorptivity coefficients of most of the compounds that were found in the effluent enabled us to calculate a mass balance that encompassed 81% of the evaporated vapor from the saturator cell during the time of the study.

Blank

PREFACE

The work described in this report was performed under the direction of the Detection Capability Officer, Defense Threat Reduction Agency Joint Science and Technology Office (DTRA JSTO). This work was started in February 2009 and completed in March 2009.

The use of either trade or manufacturers' names in this report does not constitute an official endorsement of any commercial products. This report may not be cited for purposes of advertisement.

This report has been approved for public release. Registered users should request additional copies from the Defense Technical Information Center; unregistered users should direct such requests to the National Technical Information Service.

Acknowledgments

The authors thank Dr. William Creasy (Science Applications International Corporation) and Dr. Roderick Fry (U.S. Army Edgewood Chemical Biological Center [ECBC]) for their analysis of the feedstock by nuclear magnetic resonance, and Kenneth Sumpter (ECBC) for analyzing the VX by gas chromatography–mass spectrometry. We are especially grateful to Dr. Ngai Wong (DTRA JSTO) for his continued support and encouragement of our work.

Blank

CONTENTS

1.	INTRODUCTION	11
2.	EXPERIMENTAL PROCEDURES	12
2.1	Instruments and Laboratory Apparatus	12
2.2	Analysis of Feedstock	13
2.3	Theory and Calculations	15
3.	RESULTS AND DISCUSSION	17
3.1	Prediction of Initial Composite Spectrum	17
3.2	Summary of Experimental Conditions	20
3.3	Results from the Initial Experiment	20
3.4	Quantitation of Compounds by Vapor-Phase IR: Results from the Experiments at 5 and 15 °C	22
3.5	Quantitation of Acetone by Vapor-Phase IR	24
3.6	Quantitation of DIA by Vapor-Phase IR	27
3.7	Quantitation of DICDI by Vapor-Phase IR	30
3.8	Quantitation of DEMP and VX by Vapor-Phase IR	32
3.9	Mass Balance	36
4.	CONCLUSIONS	36
	LITERATURE CITED	39
	ACRONYMS AND ABBREVIATIONS	43

FIGURES

1. Structure of O-ethyl-S-(2-diisopropylamino)ethyl methylphosphonothiolate (VX) 11

2. Saturator cell efficiency as a function of carrier rate 13

3. Composite spectrum of VX generated by applying Raoult's law predictions of the vapor pressures and absorptivity coefficients of compounds found in weapons-grade VX 19

4. Vapor-phase absorptivity coefficient of VX from PNNL database, valid at 69 °C 19

5. Spectrum of effluent from the VX-filled saturator cell 15 min after the start of the experiment 21

6. Composite spectrum of VX generated by applying Raoult's law predictions of the vapor pressures and absorptivity coefficients of compounds found in weapons-grade VX 22

7. Mass rate of acetone observed in effluent from VX-filled saturator cell on 25 February 2009 23

8. Spectrum of effluent from VX-filled saturator cell acquired on 26 February 2009 24

9. Mass rate of acetone observed in effluent from VX-filled saturator cell on 4 and 5 March 2009 25

10. Mass rate of acetone in effluent from VX-filled saturator cell on 16 March 2009 26

11. Spectrum of VX effluent and acetone reference spectrum showing a match 27

12. Mass rate of DIA observed in effluent from VX-filled saturator cell from 4 to 6 March 2009 28

13. Mass rate of DICDI observed in effluent from VX-filled saturator cell from 4 to 16 March 2009 29

14. Mass rate of DICDI observed in effluent from VX-filled saturator cell on 17 March 2009 31

15. Spectra of vapor from VX-filled saturator cell (acquired on 4 March 2009) DEMP and DIA 32

16. Spectra of vapor from VX-filled saturator cell at carrier rates of 100, 500, and 1000 sccm 33

17. Spectra of vapor from weapons-grade VX in a saturator cell at (a) 30 min and (b) 180 min 34

18. IR spectra of VX 34

TABLES

1. Summary of Results from GC-MS Analysis of VX Sample from Ton Container A49 14

2. Calculated Vapor Pressures at Temperatures of Selected Compounds Observed in Vapor from Weapons-Grade VX 18

3. Summary of Bath Temperatures and Carrier/Diluent Temperatures in the VX Vapor Experiments 20

4. Integrated Mass of DICDI from VX Experiments 25 February to 19 March 2009 32

5. Predicted Mass Rates and Absorbance Values in Vapor-Phase Spectra of Weapons-Grade VX 35

6. Mass Balance of Compounds Observed in the Vapor from the VX Saturator Cell and Gravimetric Data (Obtained from the Starting and Ending Weights of the Saturator Cell) 36

Blank

VAPOR-PHASE INFRARED SPECTRAL STUDY OF WEAPONS-GRADE O-ETHYL S-2-(DIISOPROPYLAMINO)ETHYL METHYLPHOSPHONOTHIOLATE (VX)

1. INTRODUCTION

Among the chemical warfare agents, the organophosphonates (classified as nerve agents) encompass a class of highly toxic compounds with a wide range of persistencies and toxicities. The nerve agents can be further split into three subclasses with similar structures: (1) O-alkyl *N,N*-dialkylphosphoramidocyanidate (e.g., GA or tabun); (2) alkyl alkylphosphonofluoridate (e.g., GB or sarin); or (3) O-alkyl-S-2-(dialkylaminoethyl) alkylphosphonothioate (e.g., the V-series).

This report covers a study of the infrared (IR) spectra produced by evaporation of a member of the third subclass listed in the paragraph above, O-ethyl-S-(2-diisopropylamino)ethyl methylphosphonothiolate (VX). VX has the Chemical Abstracts Service (CAS) Registry Number 57082-69-9. The molecular formula is $C_{11}H_{26}NO_2PS$, and the molecular weight is 267.37. The structure is shown in Figure 1.

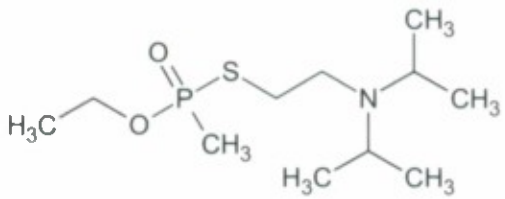

Figure 1. Structure of O-ethyl-S-(2-diisopropylamino)ethyl methylphosphonothiolate (VX).

Standoff detection systems, especially those operating in the mid-IR region of the spectra, are primarily programmed to identify chemical warfare agents on the basis of their vapor-phase IR signatures. Several of the G-series agents (subclasses 1 and 2 above) have significant vapor pressures (P) and volatilities (GB: $P_{25\,°C}$ = 2.48 torr[1]) that facilitate the detection of a vapor cloud. However, the vapor pressures and volatilities of the subclass of V agents tend to be lower than those of the G agents. VX has a vapor pressure of 0.00088 torr at 25 °C,[2] which is more than 2800 times lower than sarin. Furthermore, the vapor pressures of many of the impurities in VX are much higher than that of the pure agent. A first-order approximation would predict that impurities in VX, even at very low concentrations, could contribute to the IR signature in a manner that is disproportionate to their molar or mass concentrations. Therefore, the compound clearly presents a challenge for standoff detection. Nevertheless, with a lethal dose for 50% of the population (LD_{50}) of 5 mg,[3] the early warning of potential contamination is critically important.

2. EXPERIMENTAL PROCEDURES

2.1 Instruments and Laboratory Apparatus

The system used to generate the continuous vapor stream was an adaptation of the saturator cell method developed at the U.S. Army Edgewood Chemical Biological Center (ECBC) for measuring the volatility of chemical warfare (CW) agent related compounds.[4]

The method, which was modified to generate continuous streams of chemical compounds and obtain quantitative vapor-phase IR spectra, has been used to measure the absorptivity coefficients of a variety of chemical agent related compounds.[5–8] The saturator passes a stream of nitrogen carrier gas, which was obtained from the boiloff of a bulk liquid nitrogen tank, across an alumina Soxhlet-shaped wick positioned in a glass holder filled with the analyte. This technique yields a saturated vapor-liquid equilibrium of the analyte on the downstream side of the saturator cell at flow rates that are less than approximately 100 mL/min. When the saturator cell is suspended in a constant-temperature bath, the concentration of the analyte can be predicted by its vapor pressure at the temperature of the bath. At carrier rates >100 mL/min, the efficiency of the saturator cell will slowly decline.

Using the saturator cell and bath, we have been able to calculate the change in the vapor-liquid equilibrium (percent of saturation) as a function of the carrier rate (Figure 2) by measuring the change in mass at a range of carrier rates. The mass rate will remain constant for a pure compound (assuming that the carrier rate and temperature do not change). The carrier gas was controlled with a Brooks Model 5850S (Emerson, Hatfield, PA) mass flow controller. A second mass flow controller was used to add diluent to the stream, which provided an additional way to adjust the concentration of the compound delivered to the White cell of the Fourier transform infrared (FTIR) spectrometer. The linearity of the S-series mass flow controllers was adjusted using a second-order polynomial, which resulted in rate uncertainties of approximately 1% or better at flows ≥25% of full scale.

Spectra were obtained with a Bruker model IFS/66V FTIR. The instrument was equipped with deuterated triglycine sulfide and mercury–cadmium–telluride (HgCdTe) detectors and was capable of obtaining spectra with a maximum spectral resolution of 0.1125 cm^{-1} (unapodized). The interferograms were recorded from (15,798 to 0) cm^{-1} with a resolution of 0.5 cm^{-1}. Single-beam spectra were averaged from 128 scans. A background spectrum of the dry nitrogen was taken, the carrier was started, the vapor from the saturator cell was switched to the White cell, and the acquisition of sample spectra was started at intervals of 3 min until the carrier flow was stopped. Absorbance (log_{10}) spectra were processed with boxcar apodization and 2× zero filled to obtain a data spacing of 0.25 cm^{-1}. The instrument is equipped with a variable path White cell. The experimental data used a path length of 2.727 m. The temperature of the White cell was maintained at 23 ± 0.1 °C through the use of a thermostatically controlled chamber that enclosed the spectrometer and cell. Data were acquired at a speed of 60 kHz (helium–neon [HeNe] laser zero-crossing frequency) using the HgCdTe detector. Absorbance spectra of the vapor effluent were computed using background spectra of clean, dry nitrogen. To minimize the effects of nonlinearity in the detector, the interferograms were

processed using the proprietary Opus nonlinearity correction function. All interferograms were archived, thus enabling additional post-processing of data as needed.

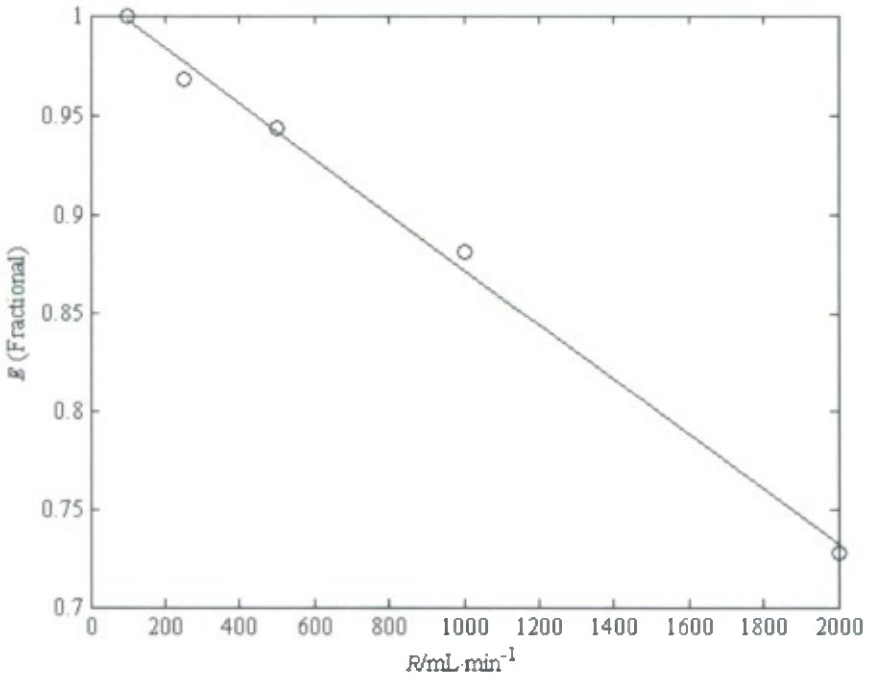

Figure 2. Saturator cell efficiency as a function of carrier rate. The equation for the fitted line above is $E = (0.0001402 \times R) + 1.012$, where E = fractional efficiency and R = carrier rate referenced to a temperature of 23 °C.

The saturator cell was weighed prior to the start of each experiment. At the end of each day's experiment, the saturator cell was dried, equilibrated for a minimum of 2 h at room temperature, and then reweighed. The change in mass was compared to the data obtained from the IR spectra of the effluent (described in Section 2.3).

Temperature and pressure data were recorded using National Institute of Standards and Technology (NIST)-traceable digital manometers and thermometers, and all data were archived.

2.2 Analysis of Feedstock

The material used to generate the vapor streams for the experiments was an archived sample from 35274-15, Ton Container A49. An aliquot of the sample was analyzed by gas chromatography–mass spectrometry (GC-MS) in split mode on 13 September 2007.[9] Results are shown in Table 1. Fractions shown in the table were computed from the areas in the GC chromatogram. Although these can provide an indication of the relative concentrations of the

compounds, the fractions are only an approximation of either mass or molar fractions of the materials.

Analysis of the vapor-phase IR spectra of the effluent from the VX showed the presence of an additional compound, acetone (which was not included in Table 1). The original source of the acetone in the sample was not determined, although suggested sources included residue from the use of acetone to rinse the ton containers or the glassware that was used to take the samples from the ton containers. Analysis by nuclear magnetic spectroscopy (NMR, ^{1}H) confirmed the identification at a mass fraction of $0.27 \pm 0.12\%$ (mol fraction $1.23 \pm 0.55\%$, with a confidence interval of approximately 95%). When the results from the GC-MS analysis were reexamined using an extracted ion, the peak for acetone was found; although the peak was too small to determine the area fraction.

Table 1. Summary of Results from GC-MS Analysis of VX Sample from Ton Container A49. Examination of the peak area fractions from the chromatogram gives only an approximation of mass or molar fractions of the individual compounds found.

Reaction Time (RT) (min)	Molecular Weight	Compound	Peak Area (%)
2.38	101	Diisopropylamine (DIA)	0.31
7.83	126	1,3-Diisopropylcarbodiimide (DICDI)	0.84
11.13	168	Diethyl methylphosphonate (DEMP)	0.10
12.17	161	2-(Diisopropylamino)ethanethiol	0.32
13.42	187	2-(Diisopropylamino)ethyl vinyl sulfide $[(iPr)_2\text{-}N\text{-}CH_2CH_2SCH{=}CH_2]$	0.07
13.65	144	*N,N'*-Diisopropylurea	0.51
14.73	189	2-Diisopropylaminoethyl ethyl sulfide	0.05
16.29	230	Diethyl dimethypyrophosphonate	1.14
18.40	251	O-Ethyl O-[2-(Diisopropylamino)ethyl] methyl phosphoric acid	0.05
20.09	267	VX	93.55
20.37	–	Unknown (base 114 *m/z*)	1.87
21.46	281	O-Ethyl S-[2-(diisopropylamino)ethyl] ethylphosphonthiolate	0.40
23.65	320	Bis[(diisopropylamino)ethyl] disulfide	0.79

2.3 Theory and Calculations

The pressure over a solution is equal to the total partial pressures of the solutes in the solution. According to Raoult's law, the partial pressure of a solute is proportional to the partial pressure of the pure solute and its molar fraction in the solution:[10]

$$P = P_a X_a + P_b X_b + P_c X_c \ldots \quad (1)$$

where P is the pressure over the solution, and $P_a X_a \ldots$ are the pressure of the pure solvent and its mole fraction. For dilute solutions with only two components, particularly when the two compounds are chemically similar, the use of Raoult's law can yield predicted pressures that are close to the actual values. In complex solutions, with a variety of intermolecular interactions, or for azeotropic solutions, pressure can only be approximated by applying Raoult's law and, in general, it needs to be determined empirically. The equation can, however, be used as a starting point for estimating the evaporation of a solution and, in this case, the solution was weapons-grade VX from a saturator cell.

As stated previously, saturator cells have been used at ECBC to measure the vapor pressure of a variety of compounds, including CW agents in the solid phase.[11] Eq 2 below is used to calculate the vapor pressure of a compound (P_a) from saturator cell measurements

$$P_a = P_{\text{sat}} \frac{n_a}{n_a + n_{\text{carrier}}} \quad (2)$$

where P_{sat} is the total pressure in the saturator cell, n_a is the number of moles of the compound (from the change in mass and molecular weight of the compound), and n_{carrier} is the number moles of carrier gas (obtained from the flow rate of the carrier and the ideal gas law)

$$n_{\text{carrier}} = \frac{FR \cdot \Delta t \cdot P}{RT} \quad (3)$$

where FR is the flow rate of the carrier in L · min^{-1}, t = time in minutes, P = 101,325 Pa, R = 8,314.5 L · Pa (mol · K)$^{-1}$, and T = the calibration temperature of the mass flow controller in Kelvin (generally 294.26 K for the mass flow controllers in our laboratory).

For low-volatility compounds, where n_{carrier}/n_a approaches 1, n_a in the lower part of the fraction in eq 2 can be ignored, and the equation can then be rearranged and combined with eq 1 to yield

$$n_a = \frac{P_a X_a n_{\text{carrier}}}{P_{\text{sat}}} \quad (4)$$

By setting t = 1 in eq 3, as long as P_a is known, and X_a = 1 (i.e., the purity of the compound in the saturator cell is 100%), eq 4 can be used to predict the evaporation rate of a compound from a saturator cell. This should be a steady state as long as P_{sat} remains constant. In most cases,

saturator cells are used to generate vapor from compounds having purities of >95%. In such cases, the concentrations of other compounds in the solution (X_a) are typically 1 to 2%, and eq 4 is a Raoult's law prediction of the *instantaneous* evaporation rate from a saturator cell. In most cases, the vapor pressures of the compounds in the solution will differ. At least for an ideal Raoult solution, examining eq 4 suggests that, regardless of the starting molar concentrations, if $P_aX_a < P_bX_b$, X_b will decrease and X_a will increase over time. As X_b decreases, its evaporation rate, n_b, will also decrease asymptotically.* In the simplest case, $f(t) = \ln(n_b)$, where $f(t)$ can be described using the relationship $at + b$, which can then be written as

$$b_0 t + b_1 = \ln(n_b) \tag{5}$$

Eq 5 can then be rewritten as

$$e^{b_0 t + b_1} = n_b \tag{6}$$

The integral of eq 6 is computed as

$$\int e^{b_0 t + b_1}\, dt = \frac{e^{b_0 t + b_1}}{b_0} \tag{7}$$

The evaporation rate of a compound (n_b) can be determined from its concentration in the vapor, which can be calculated from the IR spectra by rearranging Beer's law[12]

$$A_i(\tilde{\nu}) = a_i(\tilde{\nu}) L c_i \tag{8}$$

to obtain

$$c_i = \frac{A_i(\tilde{\nu})}{a_i(\tilde{\nu}) L} \tag{9}$$

where c_i is the concentration of compound i in the vapor, $A_i(\tilde{\nu})$ is the absorbance of the compound at a wave number, $a_i\ (\tilde{\nu})$ is the absorptivity coefficient of the compound at that wave number, and L is the path length.

Eq 9 can be computed using $A_i(\tilde{\nu})$ and a_i as either intensity at a single wave number (peak height) or integrated across a region. The reference spectra were recorded at a higher resolution (0.125 cm^{-1}) than the sample spectra. In such a case, integrating across a spectral region can improve the accuracy of the calculations. For that reason, we preferred to use integrated absorbance to calculate the concentrations of the compounds. The exceptions were (1) Acetone: An unknown compound was present in the VX with an absorption band adjacent to the ketone carbonyl stretch band of acetone. The unknown compound apparently had a low vapor pressure, and its intensity changed little over the course of the experiments. Its

* This also implies that the concentration of X_a and proportion of n_a increase gradually. Because we are considering the more typical starting case in which X_a is much larger than X_b, the proportional effect on the rate of n_a is much smaller.

concentration was apparently low, and it did not interfere with the acetone except at lower concentrations of acetone, which were then calculated using peak height. (2) DEMP: The phosphoryl band used to calculate the concentration of the compound is in a busy region of the spectrum, with bands from several other compounds nearby. Concentrations of the compound were computed using peak heights only. When peak heights were used, they were computed as means across a narrow region (≈1 to 2 cm^{-1}), to minimize the effect of noise.

The reference spectra used to calculate the concentrations of compounds in the vapor are provided in units of reciprocal micromoles per mole × meter $(\mu mol/mol)^{-1}m^{-1}$ (parts per million-meter, ppm-m), where micromoles = $MW \times 10^{-6}$ (yielding a mass in micrograms) and moles = molar volume of the diluent gas (nitrogen = 24.13 L at 294.26 K, which is the calibration temperature of the mass flow controllers). The reference spectra were normalized to 296.15 K (the temperature of the White cell used in our measurements) and 101,325 Pa. The following equation can thus be used to calculate the mass rate, R, of c_i:

$$R = \frac{c_i(FR)(MW)(P_{amb})}{24.13(101325)} \tag{10}$$

where R = instantaneous mass rate in micrograms per minute, FR = the total flow rate of carrier and diluent in liters per minute at 294.26 K and 101,325 Pa, MW = molecular weight of the compound, and P_{amb} = ambient pressure in pascals. Because acquiring 128 scans at 0.5 cm^{-1} resolution required approximately 1 min, R was actually a near-instantaneous rate. For those compounds having quantitative reference spectra, the least-squares fit of eq 5 was then calculated, substituting R for n. This yielded the coefficients b_0 and b_1 for $f(t)$ (eqs 6 and 7). If $f(t)$ could be determined for each compound in the vapor from the saturator cell, then this should permit the calculation of: $\sum\int m_i$, where m_i is the total mass of each compound evaporated from the saturator cell. In other words, we believed that it might be possible to compute a mass balance from the IR spectra that could then be compared to the gravimetric data that was obtained by weighing the saturator cell.

The data ultimately encompassed 500 spectra, from 12 experiments that were conducted over a total of more than 27 h, from which 5 compounds were identified and computed. This clearly could have been an overwhelming computational task. A customized algorithm was written in MatLab (Mathworks, Natick, MA) to perform batch processing of a number of tasks (baseline corrections of spectra, spectral integration, and Beer's law computations of concentrations), thus greatly simplifying the computations.

3. RESULTS AND DISCUSSION

3.1 Prediction of Initial Composite Spectrum

Prior to running experiments with actual VX, we attempted to predict a composite spectrum using Raoult's law and referring to a report that gave the mean concentrations of compounds found in 60 ton containers of the agent.[13] Those reported concentrations were generally similar to those in Table 1. Among the volatile compounds having available reference

spectra, the concentrations of two compounds were lower: DIA (0.14%) and DEMP (0.06%); and the concentrations of two other compounds were higher: DICDI (1.74%) and 2-(diisopropylamino)ethanethiol (0.89%). Acetone was reported at a mean concentration of 0.01%.

The absorptivity coefficient (α) of VX was obtained from the database compiled by Pacific Northwest National Laboratory (PNNL).[14] Absorptivity coefficients of other compounds were obtained from data that were acquired in our laboratory.[15] Vapor pressures were computed from a NIST vapor pressure database for acetone and DIA[16] and from ECBC data for DEMP and VX.[2,17] The vapor pressure of 2-(diisopropylamino)ethanethiol was computed using Antoine coefficients calculated from multiple sources of data[18–22] as well as vapor pressure data acquired while measuring the absorptivity coefficient of the compound in our laboratory. The vapor pressure of DICDI was calculated from coefficients that were computed from measurements of the compound. These measurements were made by: (1) Chemical Sciences Division at ECBC[23] and (2) our laboratory. The ECBC Chemical Sciences division provided vapor pressure measurements for DICDI that were similar to values reported by American Cyanamid Company (in the temperature range of 51 to 146 °C in 1962).[24] Our measurement of the vapor pressure of the compound at 15 °C was concurrent with the acquisition of the absorptivity coefficient.[15] Table 2 provides the vapor pressures of pure compounds, at the saturator cell temperatures from this work, along with the associated data sources. Figure 3 provides the composite spectrum, generated from the Raoult's law predictions of the vapor pressures of the volatile compounds (as well as VX). Figure 4 supplies the vapor-phase spectrum of VX from the PNNL database, acquired at 69 °C. Although the impurities were present at low concentrations, Raoult's law predicted that their IR signatures would be observable in the vapor.

Table 2. Calculated Vapor Pressures at Temperatures of Selected Compounds Observed in Vapor from Weapons-Grade VX. The pressures provided are for the pure compounds at the saturator cell temperatures in this work.

Compound	Vapor Pressure/Pa			Reference
	5 °C	15 °C	23 °C	
Acetone	12,088	–	–	16
DIA	3906	6613	9772	16
DICDI	153	317	543	15, 24
DEMP	10.8	25.4	48.0	17
2-(Diisopropylamino)ethanethiol	12.1	28.3	53.5	19–23
VX	0.011	0.038	0.094	2

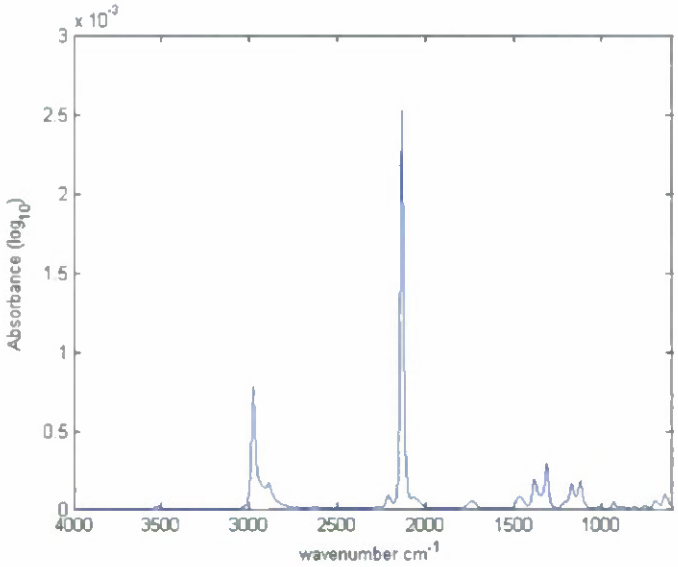

Figure 3. Composite spectrum of VX generated by applying Raoult's law predictions of the vapor pressures and absorptivity coefficients of compounds found in weapons-grade VX. Concentrations of compounds were mean values for ton containers of VX as reported in literature reference 13.

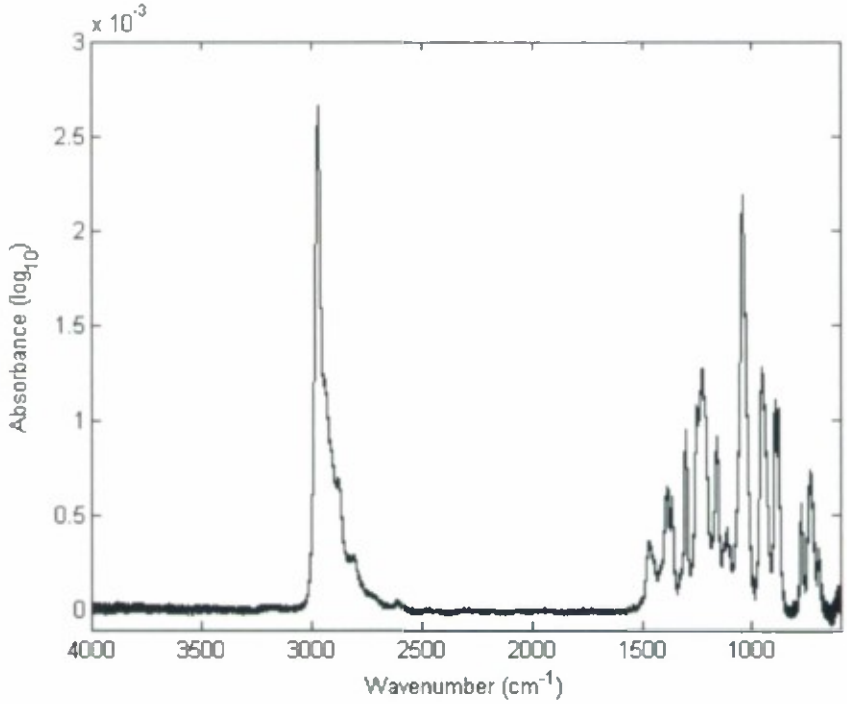

Figure 4. Vapor-phase absorptivity coefficient of VX from PNNL database, valid at 69 °C. Little or no evidence of VX is shown in the predicted spectrum of the vapor from weapons-grade VX (Figure 3).

3.2 Summary of Experimental Conditions

A total of 12 experiments were conducted between 25 February and 19 March 2009. Bath temperatures and carrier/diluent flow rates are summarized in Table 3.

Table 3. Summary of Bath Temperatures and Carrier/Diluent Temperatures in the VX Vapor Experiments.

Date(s)	Bath Temperature (°C)	Flow Rate ($cm^3 \cdot min^{-1}$ [sccm at 21.1 °C])	
		Carrier	Diluent
25 Feb 2009	5	50	2500
26 Feb 2009	15	50	2500
4–6, 10–12, 16 Mar	23	100	2500
17 Mar	23	500	2500
18 Mar	23	1000	2500
19 Mar	23	2000	2000

3.3 Results from the Initial Experiment

The first day's experiment was run at a bath temperature of 5 °C, at a carrier rate of 50 sccm (standard cubic centimeters per minute, referenced to 294.26 K), and with a diluent of 2500 sccm to capture the spectra of the higher volatility compounds present in VX, which otherwise might have purged quickly from the saturator cell. A spectrum of the effluent (acquired at 15 min into the experiment), along with the reference spectra of acetone and DICDI for comparison, are provided in Figure 5. The prominent absorption feature associated with the ketone carbonyl (C=O stretch) from acetone was unexpected, given the initial report from the GC-MS analysis of the VX sample.[9] Furthermore, evaluation of the intensity of the band indicated that the acetone was likely present at a concentration greater than the mean value of 0.01% reported in literature reference 13, which contained data that was likely to have been obtained by GC-MS analysis also.

A bias in the concentration of the acetone reported in the literature could have occurred for two reasons: (1) The numbers that were obtained during integration of a chromatogram from GC-MS analysis, represented area fractions of the peaks from the individual compounds in the sample. The peak area fractions, in turn, were calculated from the totals of the charged mass fragments detected. They were not a direct measurement of the portion of either the mass (or molar concentration) of the compounds making up the sample. Compounds that fragment similarly to one another in the electron beam may have peak area fractions that are similar to their respective molar concentrations, although this is not guaranteed. (2) To detect the presence of the compounds with the lowest boiling temperatures, GC analysis must be performed with the neat sample undiluted in solvent. This requires the GC to be operated in "split" mode, in which most of the sample that is injected into the heated liner in front of the GC column is vented to bypass the column. The low boiling temperature of acetone (56.0 °C)[25] may

have eaused mueh of the ehemieal to vaporize and expand into the liner more quiekly than the other compounds in the VX, eausing most of it to be vented.

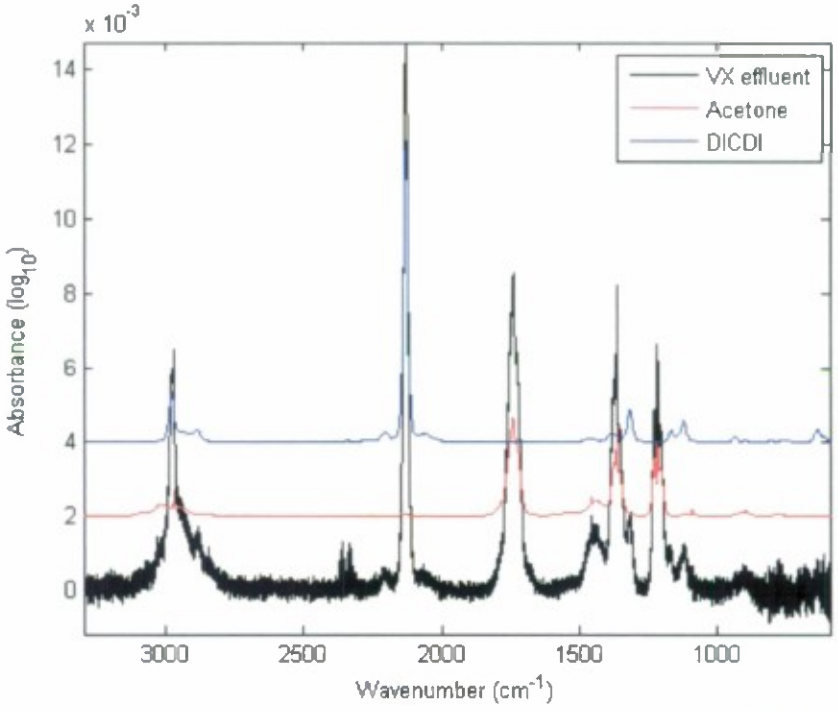

Figure 5. Speetrum of effluent from the VX-filled saturator eell 15 min after the start of the experiment. The speetrum is dominated by DICDI (2130 em^{-1}) and aeetone (1740 em^{-1}). The referenee speetra of the two eompounds have been offset for display purposes.

Aeetone at a mass or molar fraetion of 0.01% would not have been measurable by NMR. Evaluation of the intensity of the absorption features shown in Figure 5 indieated that it might, nevertheless, have been possible to deteet and measure aeetone with NMR. This was subsequently done using an internal standard method. The reported molar fraetion of 0.27 ± 0.12% for aeetone has a large uneertainty because of the relatively small size of the aeetone peak in the NMR speetrum of the VX. Nevertheless, this value, eombined with the results from GC-MS analysis,[9] provided a new starting point to prediet the speetrum of the VX.

Upon analysis, the result, shown in Figure 6, still appeared to overestimate the relative eontribution of the aeetone. There were several possible explanations for this: (1) The aetual eoneentration of aeetone eould have been on the low side of the uneertainty range reported after using the NMR. (2) The vapor pressure of aeetone in solution with VX may not have followed an ideal Raoult's law behavior. (3) The molar eoneentration of DICDI was higher than the peak area fraetion reported as a result of using the GC-MS. Unfortunately, beeause the protons in DICDI are similar to those found in VX and other nitrogen-eontaining impurities, it was not possible to obtain an independent estimate of the VX eoneentration using NMR. Therefore, the true mass or molar eoneentration of the stabilizer in the VX remained undetermined. The experienee did, however, illustrate the usefulness of a multidiseiplinary approaeh, in whieh several analytieal teehniques were used to provide pieees of the puzzle and emphasize the need for empirieal verifieations of the predietions.

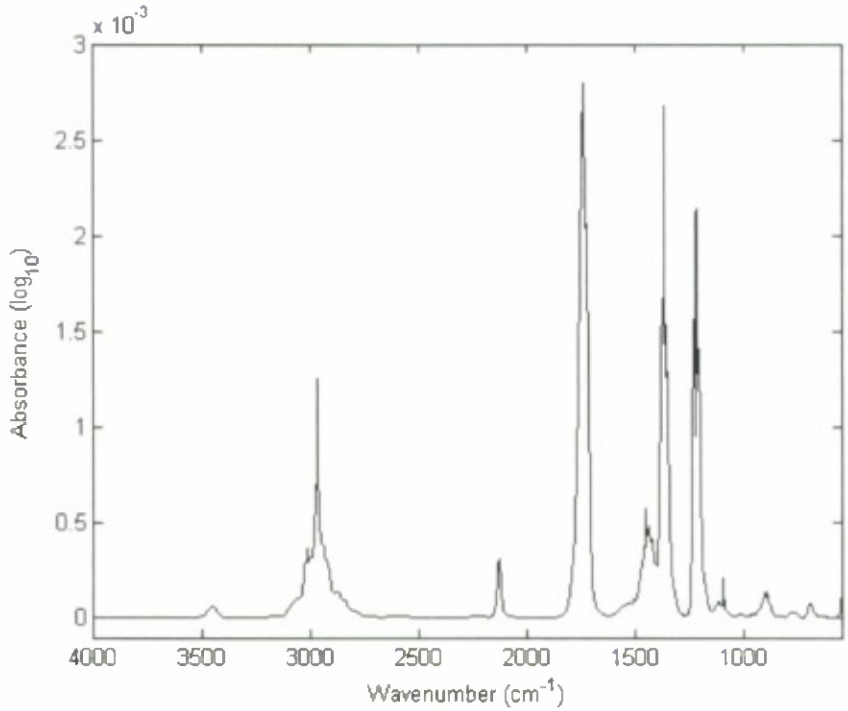

Figure 6. Composite spectrum of VX generated by applying Raoult's law predictions of the vapor pressures and absorptivity coefficients of compounds found in weapons-grade VX. The spectrum reflects the concentration of acetone observed by the use of the NMR and the concentrations of other compounds observed during GC-MS analysis (literature reference 9).

3.4 Quantitation of Compounds by Vapor-Phase IR: Results from the Experiments at 5 and 15 °C

When plotted as a function of time, the mass rate of acetone obtained during the first day's experiment appeared to exhibit the decay that was predicted in eq 5, as shown in Figure 7. The calculated mass rate of acetone at t_0 = 50.7 μg·min^{-1} decayed to 24.2 μg·min^{-1} at t = 69.5 min, which was the end of the experiment. The total mass of acetone observed (from eq 7, the integral of eq 6) was 2.5 mg. The mass rate of DICDI remained nearly constant at a mean rate of 8.8 μg·min^{-1}, resulting in a total mass of 0.6 mg. Given the peak area fraction of 0.83% for the compound and the small R value, it would have been difficult to detect its decay. The total decay for both DICDI and acetone was 3.1 mg. The change in mass obtained gravimetrically, by weighing the saturator cell at the beginning and end of the experiment, was also 3.1 ± 0.2 mg. The initial mass rate of DIA was predicted to be 25 μg·min^{-1} when Raoult's law was applied. (This prediction was made on the assumption that the GC-MS area fraction of 0.31% equaled its molar concentration.) The absorption feature of DIA (centered near 690 cm^{-1}) that was used for quantitation was weak [α = 0.00021 (μmol/mol)$^{-1}$m^{-1}, which gave a prediction of A = 0.001] and close to the detector cutoff (root mean square [RMS] noise = 0.0002 A). This was consistent with the failure to observe DIA in the vapor. Because the prediction obtained using Raoult's law for the mass rate of VX was R = 0.056 μg·min^{-1}, and a similar prediction was obtained for DEMP (R = 0.061 μg·min^{-1}), the failure to detect either of these two compounds was also expected.

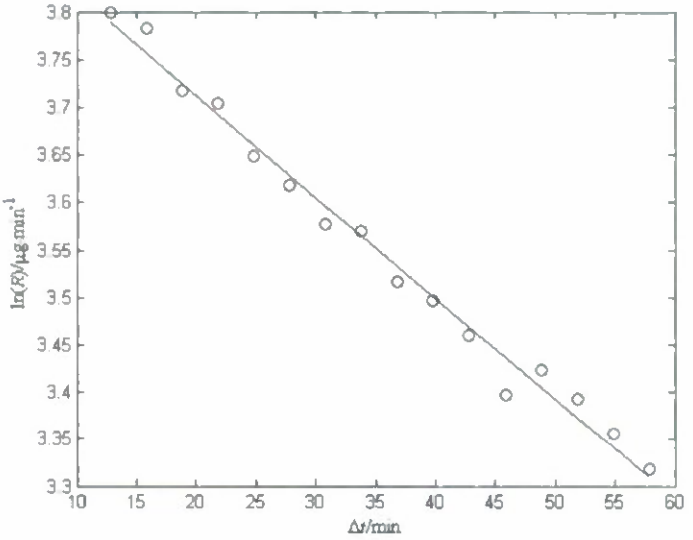

Figure 7. Mass rate of aeetone observed in effluent from VX-filled saturator eell on 25 February 2009. The deeay in aeetone output appeared to follow the behavior predieted using eq 5: $\ln(R) = b_0 t + b_1$, where $b_0 = -0.0165$ and $b_1 = 3.925$.

During the seeond day's experiment, the eonstant temperature bath was set to 15 °C, the earrier flow was operated at 50 seem, and the diluent was set to 2500 seem. The relative intensities of aeetone and DICDI were similar to those observed at 5 °C. The integrated masses of aeetone and DICDI were 2.4 and 1.8 mg, respeetively. In eontrast to the previous day's experiment, DIA was identified in the VX vapor, as shown in Figure 8, at a nearly eonstant rate of 13.5 $\mu g \cdot min^{-1}$, with an integrated mass of 0.9 mg. Assuming the results from the GC-MS analysis refleeted the molar eoneentration of DIA, and that an insignifieant fraetion of its starting mass was eonsumed during the first day's experiment, the R_{pred} was 42 $\mu g \cdot min^{-1}$. The total for aeetone, DICDI, and DIA together was 4.1 mg, whieh eontrasted with the ehange in mass of 6.9 mg from the saturator eell weight. The R_{pred} of VX was 0.20 $\mu g \cdot min^{-1}$, and the R_{pred} of of DEMP was 0.24 $\mu g \cdot min^{-1}$. The predieted total mass of both eompounds was 0.03 mg.

Throughout the series of experiments, we looked for evidenee of the 2-(diiso-propylamino)ethanethiol (VX thiol) in the VX vapor by eonsidering the following eharaeteristies of the eompound:

- Its reported area peak fraetion (from GC-MS) and pure vapor pressure were higher than those of DEMP in the sample.
- At 15 °C, and with an assumed mole fraetion of 0.31%, the R_{pred} of VX thiol was 0.30 $\mu g \cdot min^{-1}$ and total mass eonsumed would have been expeeted to have been 0.03 mg.
- Within the fingerprint region of VX, the most intense band in the absorptivity eoeffieient of VX thiol was observed at 1166 em^{-1}, with $\alpha = 0.00042$ $(\mu mol/mol)^{-1}m^{-1}$, giving a predietion of $A = 0.0002$, whieh was just equal to the RMS noise level.

- The absorption feature of VX thiol was in a crowded region of the spectrum of VX vapor; VX has a stronger band at 1160 cm^{-1}.
- DICDI has a band at 1169 cm^{-1} that is nearly as intense as VX thiol, with a weaker feature from DEMP also nearby.
- A slightly weaker absorption feature was observed for VX thiol at 1210 cm^{-1} [$\alpha = 0.00042$ $(\mu mol/mol)^{-1}m^{-1}$] that may lie within the shoulder of the bands associated with the P=O stretch.

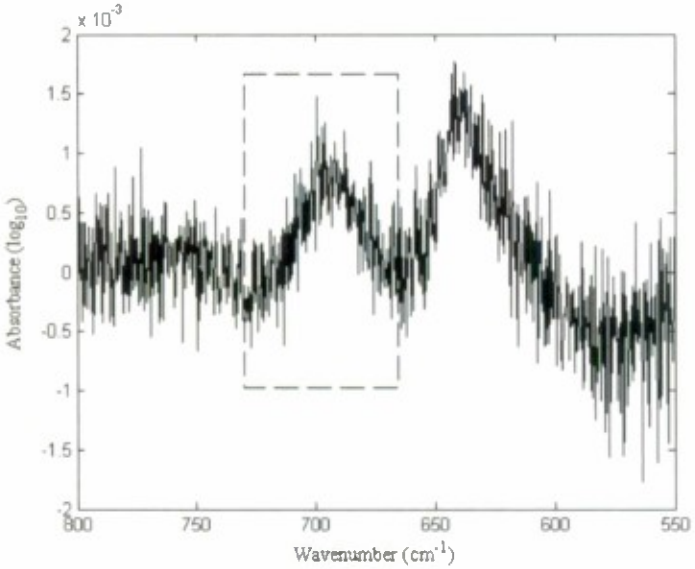

Figure 8. Spectrum of effluent from VX-filled saturator cell acquired on 26 February 2009. The rectangle highlights an absorption band near 700 cm^{-1}, which is associated with the DIA found in the vapor. The DICDI peak is at 640 cm^{-1}.

Of the remaining experiments, all were conducted with the saturator cell set to 23 °C. Among these, the next eight experiments (encompassing 4–6, 10–12, and 16–17 March 2009) were run with the carrier at 100 sccm and the diluent at 2500 sccm.

3.5 Quantitation of Acetone by Vapor-Phase IR

Among the chemicals found in VX that were not CW agents, the behavior of acetone proved to be the most interesting. Initially, the mass rate of acetone decayed rapidly at 23 °C and appeared to follow the expected logarithmic behavior. Figure 9 shows the experimental data from 4 to 5 March 2009, with R beginning at 31.4 $\mu g \cdot min^{-1}$ at $t = 0$ and declining to <1.5 $\mu g \cdot min^{-1}$ at $t = 125$ min. The apparent scattering of the data points toward the end of the plot arises from the fact that R was calculated from signals with relatively low signal-to-noise ratios (SNRs). The final data point shown in the plot was calculated from an $\int A$ in which $A_{max} = 0.0008$, in a region of the spectrum with an RMS noise level of 0.0001. As the concentration of acetone in the vapor declined, we also noted the presence of a peak centered around 1676 cm^{-1}, which was near the lower frequency shoulder of the acetone carbonyl stretch that was not associated with an acetone vibration. The frequency of the vibration would be consistent with an amide. The only compound in this class that was reported to be found in the

VX was 1,3-diisopropylurea. Based upon GC-IR spectra of the compound acquired in our laboratory, 1,3-diisopropylurea likely has a vapor-phase amide carbonyl vibration that is close to 1700 cm^{-1} and a more intense band near 1503 cm^{-1}.

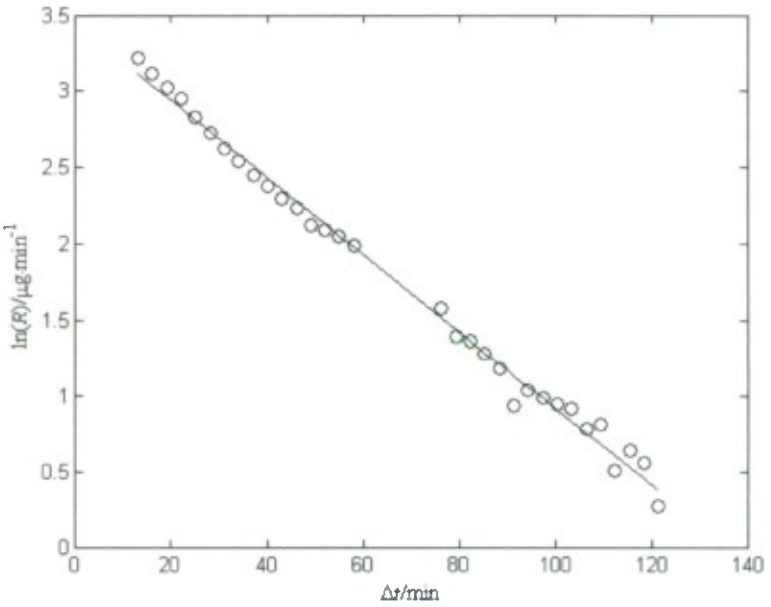

Figure 9. Mass rate of acetone observed in effluent from VX-filled saturator cell on 4 and 5 March 2009. The decay in the output of the acetone appeared to follow the logarithmic trend predicted in eq 5, with $\ln(R) = at + b$, where $a = -0.02525$ and $b = 3.446$.

On 6 March 2009, the output of acetone observed in effluent from the VX-filled saturator cell exhibited a recovery that started at 3.4 $\mu g \cdot min^{-1}$. Because an oxidation reaction to produce the acetone appeared to be unlikely, the most likely explanation for the rebound in the compound was the mass transport phenomena; i.e., the acetone was depleted at the liquid-carrier interface more quickly than it was replaced by mixing within the saturator cell. A further recovery of acetone was expected during the 4 day delay in the experiments from 6 to 10 March 2009. There was a small rebound in acetone output, from just under 0.4 $\mu g \cdot min^{-1}$ at the end of 6 March to 0.5 $\mu g \cdot min^{-1}$ at the start of the experiment on 10 March. The decay in the acetone continued on 10 and 11 March, and by 12 March the compound could no longer be detected in the vapor. The experiments were then delayed for 4 days. Although we expected that a small rebound in acetone output might be observed, when the sample was reanalyzed on 16 March, we were intrigued to note a dramatic recovery in the concentration of acetone found in the vapor from the saturator cell. This is illustrated in Figure 10, which shows that the output of acetone was nearly as high on 16 March as it was on 4 March. We considered the possibility that the absorption feature could have come from another similar compound; therefore, we verified the identity of the acetone by matching other absorption features to the reference spectrum, as shown in Figure 11. Between experiments, the saturator cell was stored in a laboratory fume hood, with the inlet and outlet ports sealed with 0.25 in. Swagelok fittings and maintained at room temperature, which did not exceed a range of 23 ± 3 °C.

At the conclusion of the experiment on 19 March, low concentrations of acetone were still detectable in the VX vapor (albeit <1 $\mu g \cdot min^{-1}$). The total integrated mass of acetone from the beginning to the end of the experiments was 6.95 mg or 0.000120 mol. The computed mass fraction was 0.092% with a molar fraction of 0.45%. At a mole fraction of 0.45%, the Raoult's law prediction yielded an initial mass rate of $R_{0/Raoult}$ = 64.3 $\mu g \cdot min^{-1}$ at 5 °C (the temperature on the first day of experimentation), compared with an experimental value of $R_{0/Exp}$ = 50.7 $\mu g \cdot min^{-1}$ (mass rate at $t = 0$ that was calculated from the equation in Figure 7).

Among the compounds studied, acetone was the only impurity for which independent confirmation of its molar fraction was available (through NMR spectroscopy). Although GC-MS offers several techniques that can provide more rigorous quantitation of trace compounds in a solution (through the use of external and internal standards, for example), such procedures are dependent upon the compounds and matrix and may require extensive methods development. Such an extended effort involving multiple compounds would have been beyond the scope of this study. Nevertheless, the availability of the NMR data, at least for acetone, proved extremely valuable for validation of the results from IR spectroscopy.

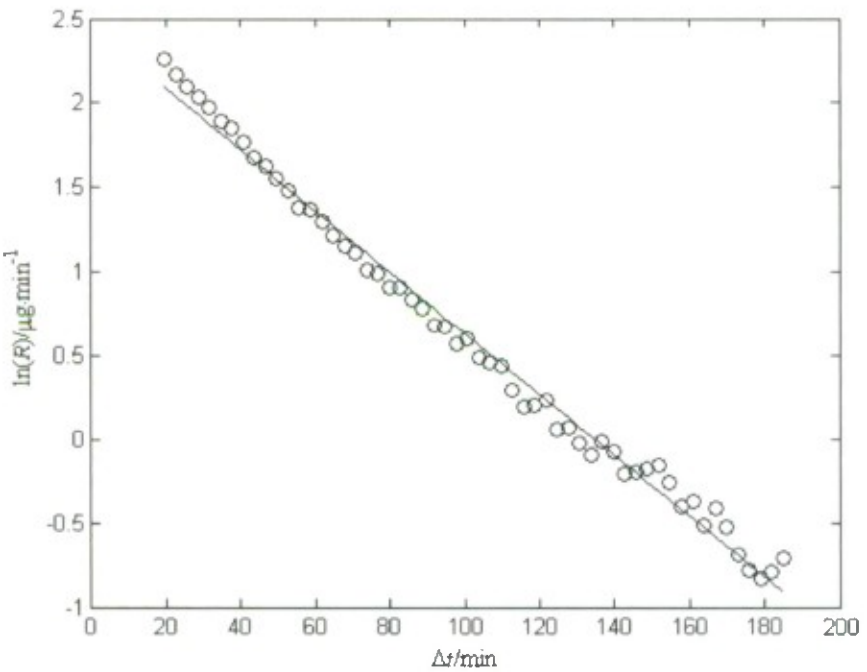

Figure 10. Mass rate of acetone in effluent from VX-filled saturator cell on 16 March 2009. Compared with the 12 March results, the acetone output exhibited a dramatic rebound.

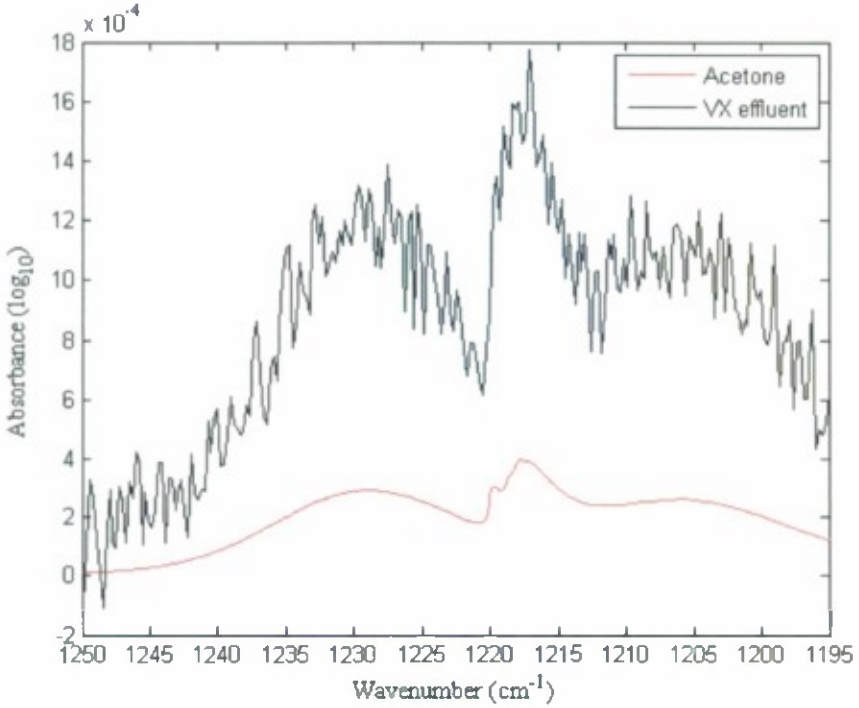

Figure 11. Spectrum of VX effluent and acetone reference spectrum showing a match.

3.6 Quantitation of DIA by Vapor-Phase IR

As noted in Table 1, DIA was detected by GC-MS analysis in the VX sample at a peak area fraction of 0.31%. If it is assumed that this value more closely approximates the molar fraction of the compound in the VX, the predicted initial mass rate at 5 °C becomes R = 24.9 $\mu g \cdot min^{-1}$, as noted in Section 3.4. Although eq 4 predicted that >1.5 mg of DIA should have evaporated from the solution during the first day's experiment, the weakness of the absorption feature precluded the possibility of detecting the compound at that temperature.

DIA was first seen in the VX vapor at 15 °C. The SNR was only 5. Nevertheless, the availability of 16 data points, the statistical advantage of signal averaging across a spectral region, and the nearly steady rate of the compound enabled us to calculate a mean rate of 13.5 ± 2.4 $\mu g \cdot min^{-1}$ and a total mass of 0.87 mg. This was significantly less than the predicted value of R = 42.2 $\mu g \cdot min^{-1}$ (assuming that an insignificant mass of DIA had been consumed on the first day).

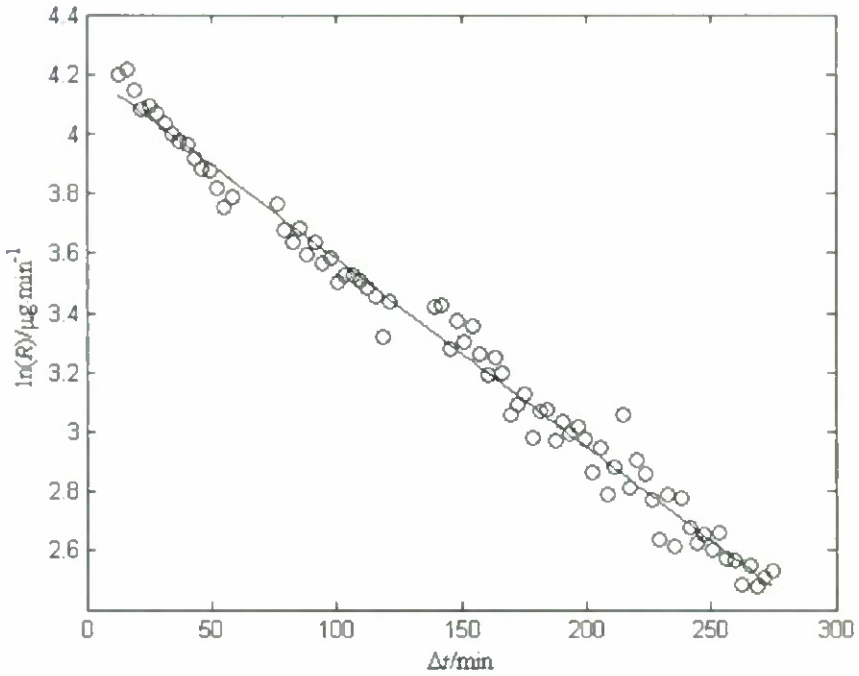

Figure 12. Mass rate of DIA observed in effluent from VX-filled saturator cell from 4 to 6 March 2009. The decay in the output of the compound appeared to follow the logarithmic trend predicted in eq 5, with $\ln(R) = b_0 t + b_1$, where $b_0 = -0.006311$ and $b_1 = 4.211$.

During the third day's experiment, with the temperature of the saturator cell set to 23 °C, the output of DIA began to follow the expected logarithmic decay, as shown in Figure 12 which contains a plot of R for the three experiments run between 4–6 March 2009. The decay equation indicates an $R_0 = 67.4\ \mu g \cdot min^{-1}$, which was five times the rate obtained at 15 °C. The integrated mass of DIA was 8.8 mg. Raoult's law predicted an increase proportional to the change in the vapor pressure of the pure compound, 9772 Pa/6613 Pa = 1.47, which was more than three times greater than the ΔR observed. A rebound effect similar to that observed with the acetone was possible, and the grouped data points from the experiments run on the 3 days appear to reflect a tendency for the rate of the compound to "recover" slightly at the beginning of the operations on 5 and 6 March. However, nitrogen-containing compounds, particularly at low concentrations and carrier flows, also tend to be "sticky" in our system and required significantly more time to passivate than was indicated by the mixing rate. It is more likely, therefore, that the data from the operations at 5 and 15 °C underestimated the mass of DIA. Starting on 6 March, the total time of each run was increased, which gave the more difficult compounds additional time to equilibrate in the White cell.

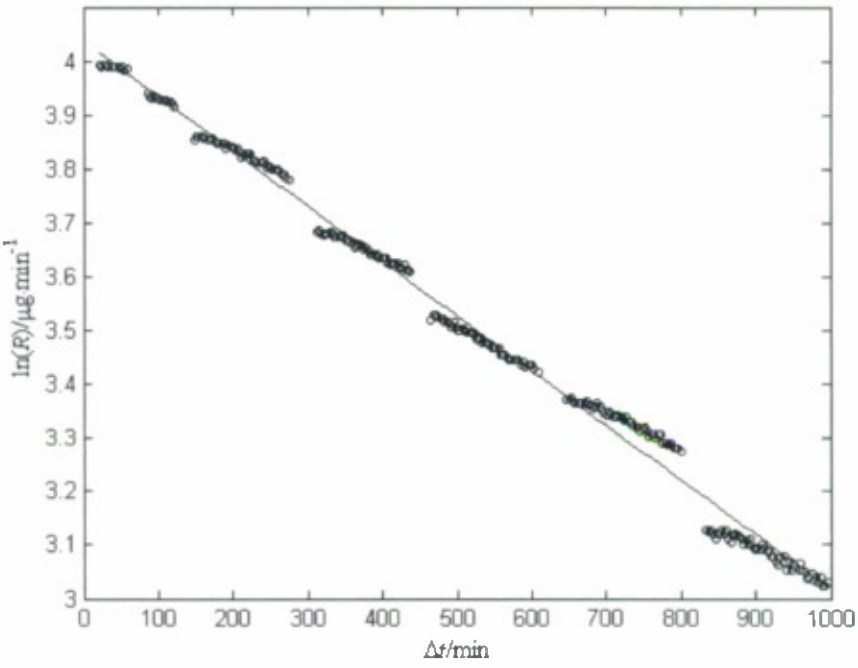

Figure 13. Mass rate of DICDI observed in effluent from VX-filled saturator cell from 4 to 16 March 2009. The decay in the output of the compound appeared to follow the logarithmic trend predicted in eq 5, with $\ln(R) = b_0 t + b_1$, where $b_0 = -0.001018$ and $b_1 = 4.0358$ and $t_{1/2} = 680.7$ min.

A more evident rebound effect was observed when the mass rate of DIA approximately doubled between the end of the operation on 6 March and the start of the experiment on 10 March 2009. The integrated mass of the DIA from the two experiments performed on 10 and 11 March was 3.8 mg. After 11 March, the compound was no longer detectable in the VX vapor.

The total observed mass of DIA from all experiments was 13.5 mg, which was equivalent to a mass fraction of 0.18%. Based upon its retention time, the unknown compound in Table 1 (RT = 20.37 min) was probably bis[S-(2-diisopropylamino)ethyl] methyl phosphonodithiolate (VX bis). Assuming the peak area fractions in Table 1 more closely approximate molar fractions, the mean molecular weight of the VX sample was 266.4. The calculated starting molar fraction of the DIA was then 0.47%, which gave a predicted value of R = 37.9 $\mu g \cdot min^{-1}$ at the beginning of the experimental series (T = 5 °C). Although a minimum detection limit for DIA was not calculated, we believe it to have been <13 $\mu g \cdot min^{-1}$. The failure to detect this compound in the VX vapor at a bath temperature of 5 °C indicates that the partial pressure and mass rate may have been suppressed in the solution more than a simple Raoult's law calculation would have predicted. Even at 23 °C, the initial mass rate of the DIA was less than two times that predicted at a temperature of 5 °C.

3.7 Quantitation of DICDI by Vapor-Phase IR

When acquiring the vapor-phase absorptivity coefficient of DICDI, we found that, similar to the testing of other nitrogen compounds, DICDI required more time than other less "sticky" compounds to equilibrate in our system. It did, however, have a strong [$\alpha = 0.00805$ $(\mu mol/mol)^{-1}m^{-1}$], narrow absorption feature near 2130 cm^{-1} in an uncrowded region of the IR spectrum. Those properties made DICDI a good compound for quantitation using IR spectroscopy, and allowed us to compute the concentration of the compound for the full series of spectra using the integrated absorbance across the band. Because of the relatively high concentration compared with the other volatile compounds (peak area fraction by GC-MS = 0.84%), DICDI was observed at a high SNR ratio (183), even at the end of the series of experiments. In fact, evaluation of the data from the first day's experiment at a saturator cell temperature of 5 °C indicated that the starting molar concentration of the compound in the VX may have been >2%.

As noted in Section 3.4, the mass of DICDI (computed from the vapor-phase IR spectra) totaled 2.4 mg during the first two experiments at 5 and 15 °C.

The experiments conducted from 4 to 16 March 2009 were all run with a carrier rate of 100 sccm and a saturator cell temperature of 23 °C. In accordance with eq 5, we expected to see a logarithmic decay in the mass rate of the compound, similar to the behavior observed with the acetone and DIA. However, contrary to our expectation, when each day's experiments were plotted separately, they appeared initially to follow a linear behavior. Although this linear behavior seemed unlikely, the results from each day's experiments were computed individually, resulting in a total mass of 35.8 mg for the seven experiments. After the final experiment was completed at a carrier rate of 100 sccm, the pooled data appeared to exhibit the predicted logarithmic trend, as shown in Figure 13 (Section 3.6). Using the equation of the fitted line in Figure 13, the integrated mass of the pooled data, $\int_0^{997} f(t) = 35.4$ mg, little had changed from the mass that was obtained by computing the experiments individually. The half-life of the compound under the experimental conditions was 680.7 min. The hook-shaped appearance in the early part of the data from each day's run reflects the additional equilibration time required for the DICDI, which has two nitrogen atoms per molecule.

For the final set of three experiments beginning on 17 March 2009, carrier flow rates >100 sccm were used. As described in Section 2.1, higher flow rates reduce the efficiency of the saturator cell. In such cases, eq 4 must be rewritten to account for the reduced efficiency of the saturator cell at the higher flow rate

$$n_a = \frac{P_a X_a n_{\text{carrier}}}{P_{\text{sat}}} E \qquad (11)$$

where E is the efficiency of the saturator cell (from Figure 2). Because eq 11 encompasses a dynamic environment, it is used to predict the instantaneous mass rate of a compound only. As

we have observed through working with other compounds at high carrier rates, the decay of a volatile impurity in a compound does not necessarily follow a first-order trend with respect to the natural logarithm of its mass rate. As the carrier rate increases, the phenomenology of mass transport from the bulk liquid to the wick and then to the vapor-phase presumably becomes more complex, leading to the depletion of the more volatile compounds at the interface between the liquid and vapor. This trend is depicted in Figure 14, which shows a graph of the mass rate of DICDI on 17 March 2009, obtained at a carrier rate of 500 sccm. The mass rate of the compound on 18 and 19 March 2009 followed a similar trend.

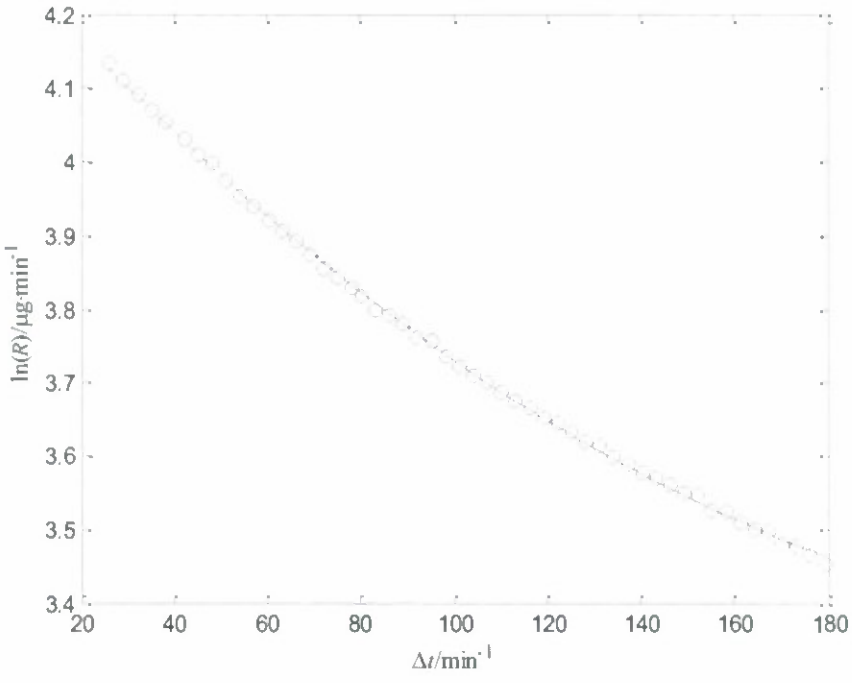

Figure 14. Mass rate of DICDI observed in effluent from VX-filled saturator cell on 17 March 2009. The decay in the output of the compound followed the trend $\ln(R) = b_0t^2 + b_1t + b_2$, where $b_0 = -0.00001299$, $b_1 = -0.006986$, and $b_2 = 4.2991$. Total integrated mass was 8.5 mg.

Table 4 lists the integrated mass of DICDI for all experiments performed in this study. As noted previously, the absorption band for the compound, even at the end of the final experiment, was still at an SNR >10. The 57.4 mg shown in the last column of the table does not, therefore, represent the original starting mass of DICDI in the VX. A better estimate of the total DICDI starting mass, found in the sample of VX in the saturator cell, could be obtained by combining (1) the masses from the first two experiments on 25 and 26 February 2009, and (2) the mass obtained by extending and integrating the equation for Figure 13 out to 10 half-lives (at which point the mass rate would have decayed to $0.5^{10} = 0.00098$ of the starting rate). This resulted in a total starting mass of 0.6 + 1.8 + 55.8 = 58.2 mg, which is a molar fraction of 1.6 %. At this concentration, the Raoult's law prediction of the partial pressure at 5 °C was 2.2 Pa, and the predicted initial mass rate of DICDI at 50 sccm carrier (the conditions of the first experiment) was $R_0 = 6.3$ µg·min^{-1}, compared with the observed rate of 8.8 µg·min^{-1}.

Table 4. Integrated Mass of DICDI from VX Experiments, 25 February to 19 March 2009.

Date	25 Feb	26 Feb	4–16 Mar	17 Mar	18 Mar	19 Mar	Total
Mass (mg)	0.6	1.8	35.4	8.5	7.1	4.0	57.4

3.8 Quantitation of DEMP and VX by Vapor-Phase IR

As noted earlier, neither DEMP nor VX was observed spectroscopically at saturator cell temperatures of 5 or 15 °C. The conditions used in the experiments run from 4 to 16 March 2009 included a saturator cell temperature of 23 °C with a carrier rate of 100 sccm and a diluent rate of 2500 sccm. The predicted mass rates were 1 and 0.3 $\mu g \cdot min^{-1}$ for VX and DEMP, respectively. Even though both compounds have strong absorption features near 1040 cm^{-1}, such low mass rates would be expected to result in a value of $A \approx 0.0002$ for the two compounds combined. Furthermore, DIA has a partially overlapping band with a maximum at 1020 cm^{-1}. At an RMS noise level of 0.0001 within the spectral region, such a low signal would have been expected to be difficult to detect. This is reflected in Figure 15, which illustrates the challenge of confirming the presence of the two phosphorous compounds.

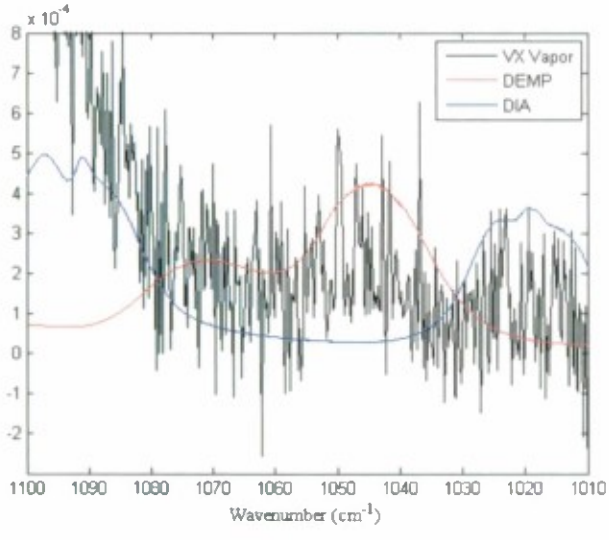

Figure 15. Spectra of vapor from VX-filled saturator cell (acquired on 4 March 2009), DEMP and DIA. At a predicted value of $A = 0.0002$ for the most intense absorption band, the presence of the two phosphorous compounds would have been difficult to confirm spectroscopically.

As the carrier rate was increased to 500 sccm and then to 1000 sccm, the presence of DEMP was clearly detectable on the basis of the P=O stretch at 1269 cm^{-1} and the P-O-C stretch in the 1000 cm^{-1} region. Figure 16 shows a comparison of the P-O-C stretching bands in spectra acquired on successive days at carrier rates of 100, 500, and 1000 sccm. Integrated masses for the experiments run with carrier rates of 500 and 1000 sccm were 0.3 and 1.0 mg on 17 and 18 March, respectively. Based upon the appearance of the bands shown in Figure 16 and the lack of a P=O band from VX, the bands shown in the figure likely resulted from DEMP.

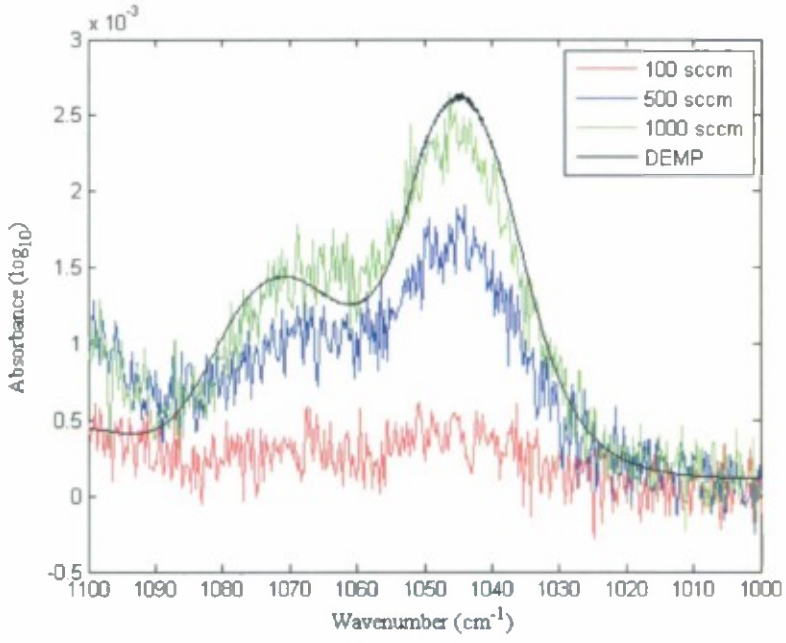

Figure 16. Spectra of vapor from VX-filled saturator cell at carrier rates of 100, 500, and 1000 sccm. The spectra, which were acquired at 30 min into each experiment, reflect the increasing concentration of DEMP at the higher carrier rates. The shape of the bands in this region, as well as the absence of a P=O band from VX (not shown above), indicate that the features likely do not show the presence of VX in the spectra.

The final experiment was run at a carrier and diluent rate of 2000 sccm. By using the high carrier rate, we hoped to increase the evaporation of VX from the saturator cell and reduce the equilibration time in our system by providing a more efficient sweep of the transfer lines and White cell. Analysis of the spectra taken at 30 and 180 min into the experiment (Figure 17) indicate that the high flow rates effectively increased the downstream concentration of VX and permitted the detection and identification of the compound in the spectra. The identification of VX was facilitated by (1) the presence of the P=O absorbance bands from both DEMP (1270 cm^{-1}) and VX (1250 cm^{-1}) at frequencies with little overlap, and (2) the change in appearance of the bands in the 1000 cm^{-1} region. The DEMP band has a shoulder at 1070 cm^{-1}, in contrast to VX, which has only the single band at 1045 cm^{-1}. Even at the higher flow rate, VX was still a "sticky" compound, and the increase in the intensities of the P-O-C bands between 30 and 180 min can easily be seen, along with a further change in their overall shape to a more VX-like appearance. The arrows shown in Figure 17a and b indicate the presence of an absorption feature in the reference spectrum near 1228 cm^{-1} that was not seen in the spectra of the vapor from the saturator cell. Evaluation of the GC-IR (vapor-phase) spectra of VX, acquired in our laboratory, (Figure 18) have indicated that the lower frequency band, if present in the vapor-phase spectrum of the compound, is much weaker than that seen in the reference spectrum (Figure 17). The lower frequency band in the VX reference spectrum, which matches the frequency of the P=O band in liquid-phase VX, likely arose from aerosolized VX in the vapor used to generate the spectrum. Furthermore, the observed $\Delta\tilde{\nu}$ of ≈20 cm^{-1} in the

frequency of the P=O band in the vapor compared with the liquid-phase spectrum of an alkylphosphonate is typical of other compounds.[26,27]

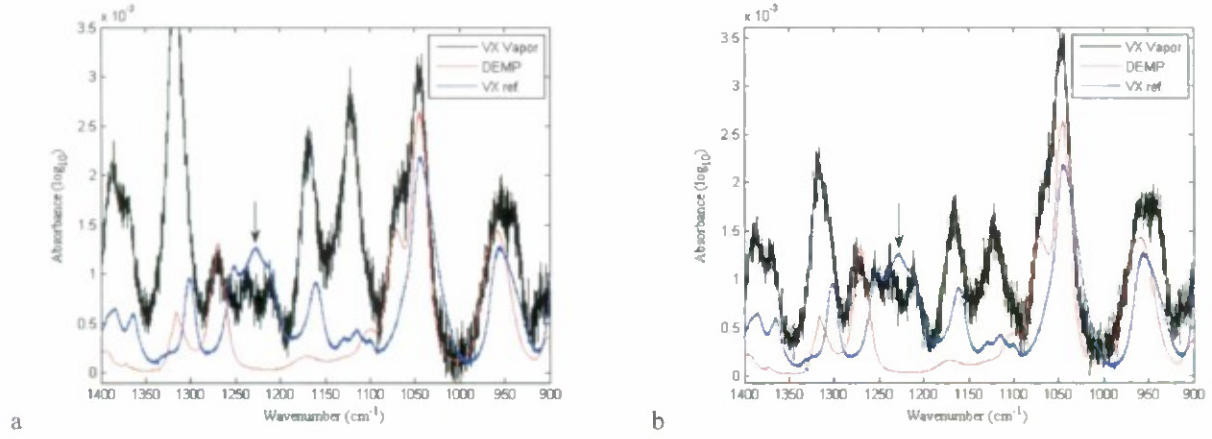

Figure 17. Spectra of vapor from weapons-grade VX in a saturator cell at (a) 30 min and (b) 180 min. The figures include the vapor-phase reference spectra of DEMP (ECBC) and VX (PNNL). The arrows highlight an absorption feature in the VX reference spectrum, apparently associated with aerosolized VX, that was absent in the spectrum of the material generated using a saturator cell.

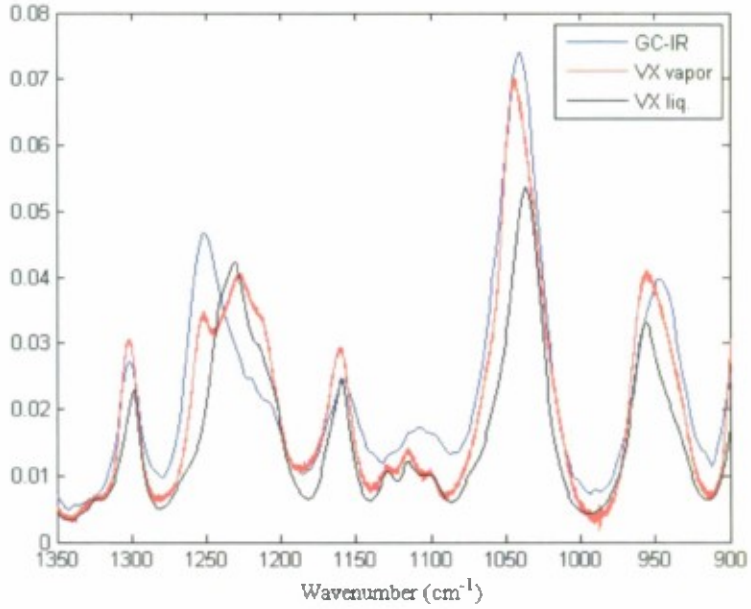

Figure 18. IR spectra of VX. The P=O stretching band in the GC-IR (vapor-phase) spectrum (blue band) was near 1250 cm^{-1}. This contrasts with the liquid-phase spectrum (black band), in which the band was near 1228 cm^{-1}. The vapor-phase absorptivity coefficient of VX from the PNNL database (red band) appears to exhibit P=O absorption features from both liquid and vapor-phase VX.

The predicted values for the mass rate and absorbance of the two compounds in the final experiment are shown in Table 5. Because the vapor pressures of the compounds have been well established by measurements conducted at ECBC,[2,17] the prediction uncertainty for R is primarily dependent upon (1) deviations from Raoult's law, which must be determined empirically, and (2) uncertainties in the concentrations of DEMP and VX. We can assume that the purity of the VX is probably at least close to the value reported by using the GC-MS. For DEMP, however, the relationship between the area fraction reported by using the GC-MS and the mass or mole fraction is unknown. Under the assumption that the fragmentation of VX and DEMP by the electron beam and the chromatographic behavior of the two compounds were similar, we used the peak area fraction from the GC-MS analysis to compute a mass fraction for the DEMP.

The vapor-phase absorptivity coefficient of DEMP has been measured by the personnel at PNNL[14] and ECBC.[15] Within the region that includes the 1045 cm^{-1} band, deviations between the data from the two laboratories was only 2.7%. Therefore, the uncertainty in the α value of the compound has little effect on the uncertainty of the predicted value of A. There has been no interlaboratory comparison of the vapor-phase absorptivity coefficient of VX. The metadata file associated with the data contains uncertainties of: Type A = 9.5% and Type B <10%. A note in the file indicates that, "some liquid probably condensed on White cell mirrors." As we have further noted, this appears to be confirmed by the appearance of the spectra within the fingerprint region. The Type B uncertainty that was reported may, therefore, be an optimistic finding. In addition to the DEMP and VX, VX thiol has a maximum absorption band at 1069 cm^{-1} with a shoulder that extends beyond 1045 cm^{-1} and likely contributes at least weakly to the spectra in Figure 17. Given the associated uncertainties, the prediction values in the last column of Table 5 are remarkably similar to the actual spectra.

Table 5. Predicted Mass Rates and Absorbance Values in Vapor-Phase Spectra of Weapons-Grade VX. The values shown in the table are for the experiment conducted at a carrier rate of 2000 sccm. The values reflect the intensities of the band at 1045 cm^{-1} that should be contributed by DEMP and VX at the predicted mass rates shown.

Compound	R (μg·min^{-1})	A ($\log_{10}$)
DEMP	4.4	0.0012
VX	15.0	0.0018

The integrated mass of DEMP from the experiments in which the presence of the compound could be identified and quantified (17–19 March 2009) was 2.6 mg. On the basis of the relationship between the P-O-C and P=O bands, and the contribution to the P-O-C band from DEMP, the mass of VX observed on 19 March 2009 was calculated to be 2.7 mg. Assuming ideal Raoult behavior and a starting molar fraction of 0.1% DEMP, the computed mass of DEMP from the experiments run 25 February to 16 March was 1.5 mg, with a total of 4.0 mg for all experiments.

3.9 Mass Balance

Table 6 provides the computed mass balance for all compounds having available spectral data. The total shown for DICDI reflects the integrated masses from the first two experiments and the calculated mass of the compound, assuming the equation in Figure 13 was used to integrate to 10 half-lives. The masses of DEMP and VX include both integrated spectral data and assumptions from Raoult's law for experiments in which the spectral signatures were too weak to be detected. The total mass of the compounds shown in Table 6 was 88.2 mg, compared with a gravimetrically determined change in mass of 108.8 mg (calculated from the difference between the starting weight of the filled saturator cell on 25 February and the ending weight on 19 March). The compounds listed in Table 6 accounted for 81.0% of the gravimetric mass change over the experimental time.

Table 6. Mass Balance of Compounds Observed in the Vapor from the VX Saturator Cell and Gravimetric Data (Obtained from the Starting and Ending Weight of the Saturator Cell).

Compound	Acetone	DIA	DICDI[a]	DEMP[b]	VX[c]	Total	Gravimetric Change
Mass (mg)	7.0	13.5	58.2	4.0	5.5	88.2	108.8

[a]Assumes data from 4 to 16 March 2009 extended to 10 half-lives

[b]Includes integrated spectral data from 17 to 19 March 2009 and assumes ideal Raoult's law behavior from 25 February to 16 March 2009

[c]Includes spectral data for 19 March 2009 and assumes ideal Raoult's law behavior from 25 February to 18 March 2009

We were unable to identify a unique absorption band of sufficient intensity under the experimental conditions for quantitation of VX thiol. Therefore, because we had no means to estimate its deviation from ideal Raoult's law behavior, we did not compute the evaporation of the compound from the saturator cell. Other compounds (listed in Table 1) may have contributed to the vapor from the VX, but were not considered in this report or shown in Table 6 because, to our knowledge, neither the quantitative vapor-phase reference spectra nor the vapor pressure data within the range of our tests were available. The compounds that most likely contributed at least part of the mass in the VX vapor included 2-(diisopropylamino)ethyl vinyl sulfide, 1,3-diisopropylurea, and diethyl methylpyrophosphonate (VX pyro).

4. CONCLUSIONS

Weapons-grade VX contains stabilizers and impurities with pure component vapor pressures that vary from that of VX by more than 6 orders of magnitude. The wide range of volatilities means that partial pressures for even trace impurities may be many times higher than that of the CW agent. When the agent is vaporized through evaporation, a complex mixture of materials results and, therefore, the spectral signatures are dominated by the more volatile compounds rather than by the VX. If the concentrations, identities, and pure component vapor pressures of the impurities in VX are known, and if reference spectra for these compounds are

available, it is possible to generate an artificial spectrum of the vapor that more closely approximates the actual vapor-phase spectral signature of the agent.

Using relatively simple mathematical procedures based upon Raoult's and Beer's laws, we were able to use vapor-phase IR spectroscopy to obtain the mass balance of the compounds that evaporated from weapons-grade VX. We were also able to determine the starting concentrations of several impurities in the agent that were difficult to measure by other analytical techniques.

Blank

LITERATURE CITED

1. Penski, E.C. *The Properties of 2-Propyl Methylfluorophosphonate (GB) I. Vapor Pressure Data Review and Analysis*; ERDEC-TR-166; U.S. Army Chemical and Biological Defense Command: Aberdeen Proving Ground, MD, June 1994; UNCLASSIFIED Report (AD-B187 225).

2. Buchanan, J.H.; Buettner, L.C.; Butrow, A.B; Tevault, D.E. *Vapor Pressure of VX*; ECBC-TR-068; U.S. Army Edgewood Chemical Biological Center: Aberdeen Proving Ground, MD, 1999; UNCLASSIFIED Report (AD-A371 297).

3. *Potential Military Chemical/Biological Agents and Compounds*; FM 3-11.9; U.S. Army Training and Doctrine Command: Fort Monroe, VA, January 2005; UNCLASSIFIED Field Manual.

4. Tevault, D.; Keller, J.; Parsons, J. Vapor Pressure of Dimethyl Methylphosphonate (AD-E491 779). In *Proceedings of the 1998 ERDEC Scientific Conference on Chemical and Biological Defense Research, 17–20 November 1998*; ECBC-SP-004; U.S. Army Edgewood Chemical Biological Center: Aberdeen Proving Ground, MD, 1999, UNCLASSIFIED Report (AD-A375 171).

5. Williams, B.R.; Samuels, A.C.; Miles, R.W.; Hulet, M.S.; Ben-David, A. ECBC Quantitative Vapor-Phase Infrared Spectral Database. In *Proceedings of the 2007 Scientific Conference on Chemical & Biological Defense Research, 13–15 November 2007*; SOAR-07-20; Chemical, Biological, Radiological & Nuclear Defense Information Analysis Center: Gunpowder, MD, 2008.

6. Williams, B.R.; Samuels, A.C.; Miles, R.W.; Hulet, M.S. *Vapor-Phase Absorptivity Coefficient of Cyclohexyl Isothiocyanate*; ECBC-TR-637; U.S. Army Edgewood Chemical Biological Center: Aberdeen Proving Ground, MD, July 2008; UNCLASSIFIED Report (AD-A485 730).

7. Williams, B.R.; Samuels, A.C.; Miles, R.W.; Hulet, M.S.; Berg, F.J.; McMahon, L.; Durst, H.D. *Vapor-Phase Absorptivity Coefficient of Bis-(2-Chloroethyl) Sulfide*; ECBC-TR-638; U.S. Army Edgewood Chemical Biological Center: Aberdeen Proving Ground, MD, July 2008; UNCLASSIFIED Report (AD-A487 002).

8. Williams, B.R.; Samuels, A.C.; Miles, R.W.; Hulet, M.S.; Berg, F.J.; McMahon, L.; Durst, H.D. *Vapor-Phase Absorptivity Coefficient of 2-Chlorovinyl Dichloroarsine*; ECBC-TR-667; U.S. Army Edgewood Chemical Biological Center: Aberdeen Proving Ground, MD, January 2009; UNCLASSIFIED Report (AD-A493 633).

9. Sumpter, K.B. *GC/MSD Characterization of VX Ton Container A49*; Memorandum dated 13 September 2007, Chemical Scienees Team; U.S. Army Edgewood Chemical Biologieal Center: Aberdeen Proving Ground, MD.

10. Ebbing, D.D. *General Chemistry*; 2nd ed.; Houghton Mifflin: Boston, 1987.

11. Buchanan, J.H.; Buettner, L.C.; Tevault, D.E. Vapor Pressure of Solid Bis(2-Chloroethyl) Sulfide. *J. Chem. Eng. Data* **2006**, *51*, 1331.

12. Griffiths, P.R.; deHaseth, J.A. *Fourier Transform Infrared Spectrometry*; 2nd ed.; Wilcy Interscience: Hoboken, NJ, 2007.

13. Magee, R.S.; Berkowitz, J.B.; Dyer, G.H.; Harper, F.T.; Heintz, J.A.; Hoeeke, D.A.; Kosson, D.S.; Walter, G.M.; Mushkatel, A.H.; Oden, L.; Parshall, G.W.; Pye, L.D.; Staehle, R.W.; Tumas, W. *Review and Evaluation of Alternative Chemical Disposal Technologies*; National Aeademy Press: Washington, DC, 1996.

14. *DOE/PNNL Infrared Spectral Library, Release 11.0*; [DVD-ROM]; Pacific Northwest National Laboratory: Riehland, WA, September 2006.

15. *ECBC Quantitative Infrared Database, Version 1.0*; U.S. Army Edgewood Chemieal Biological Center: Aberdeen Proving Ground, MD, 2009; Available on CD-ROM through the Chemieal, Biologieal, Radiologieal, Nuelear Information Analysis Center: Aberdeen Proving Ground, PO Box 106, Gunpowder, MD 21010-0106; UNCLASSIFIED.

16. *NIST TRC Vapor Pressure Database: Standard Reference Database 87*; [Computer program distributed on portable media]; National Institute of Standards and Teehnology: Gaithersburg, MD, 2001.

17. Butrow, A.B.; Buehanan, J.H.; Tevault, D.E. Vapor Pressure of Organophosphorus Nerve Agent Simulant Compounds; *J. Chem. Eng. Data* **2009**, *54* (6), 1876–1883.

18. Ratsehinskii, F. Iu.; Slavaehevskaia, N.M.; Ioffe, D.V. ß-Mereaptoethylamine and lts N-Substituted Derivatives; *Zh. Obshch. Khim.* (Engl. Transl.) **1958**, *28*, 2998.

19. Eastman Kodak Co., U.S. Patent 3,232,936, 1965.

20. Givaudan and Cie., German Patent DE 2,735,459, 1978.

21. Eastman Kodak Co., U.S. Patent 3,236,843, 1962.

22. Davis, F.A.; Ray, J.K.; Kasperowiez, S. 8-(N,N-Dialkyamino)ethyl Arylthiosulfonates: New Simulants for 0-Ethyl S-[2-(Diisopropylamino)ethyl] Methylphosphonothioate. *J. Org. Chem.* **1992**, *57*, 2594.

23. Butrow, A.B. *DICDI DSC Data*; Chemical Sciences Division, U.S. Army Edgewood Chemical Biological Center: Aberdeen Proving Ground, MD, Email, 15 April 2009.

24. U.S. Army Edgewood Biological Chemical Center: Aberdeen Proving Ground, MD, September 13, 1962, Letter from Edward Groth, Jr., American Cyanamid Co.: Bound Brook, NJ, to H. V. Rouse, Jr.

25. Lide, D.R., Ed. *CRC Handbook of Chemistry and Physics, 75th Edition*; CRC Press: Boca Raton, FL, 1994.

26. Thomas, L.C. *Interpretation of the Infrared Spectra of Organophosphorous Compounds*, Heyden & Son Ltd: New York, 1974.

27. McGarvey, D.J.; Stuff, J.R.; Williams, B.R. Vapor-Phase Infrared Spectral Study of the Analogs of the Nerve Agent Sarin. *Spectrosc. Lett.* **2000**, *33*, 795.

Blank

ACRONYMS AND ABBREVIATIONS

CAS	Chemical Abstracts Service
CW	chemical warfare
DEMP	diethyl methylphosphonate
DIA	diisopropylamine
DICDI	1,3-diisopropylcarbodiimide
ECBC	U.S. Army Edgewood Chemical Biological Center
FTIR	Fourier transform infrared spectroscopy
GC-IR	gas chromatograph–infrared analyzer
GC-MS	gas chromatograph–mass spectrometer
HeNe	helium–neon
HgCdTe	mercury–cadmium–telluride
IR	infrared
NIST	National Institute of Standards and Technology
NMR	nuclear magnetic resonance
PNNL	Pacific Northwest National Laboratory
rms	root mean square
SNR	signal-to-noise ratio
VX bis	bis[S-(2-diisopropylamino)ethyl] methyl phosphonodithiolate
VX thiol	2-(diisopropylamino)ethanethiol
VX pyro	diethyl methylpyrophosphonate